GA-A24388

VALIDATION OF THE PHYSICS MODEL FOR ECCD IN THE DIII-D TOKAMAK AND ITS APPLICATION TO ITER

by
R. PRATER, C.C. PETTY, R.W. HARVEY, J.M. LOHR,
T.C. LUCE, and M. CHOI

JULY 2003

DISCLAIMER

GA-A24388

VALIDATION OF THE PHYSICS MODEL FOR ECCD IN THE DIII-D TOKAMAK AND ITS APPLICATION TO ITER

by
R. PRATER, C.C. PETTY, R.W. HARVEY[£], J.M. LOHR,
T.C. LUCE, and M. CHOI

This is a preprint of a paper to be presented at the IAEA Technical Meeting on ECRH Physics and Technology for ITER, Kloster Seeon, Germany, July 14-16, 2003, and to be printed in the *Proceedings*.

[£]*CompX, Del Mar, California*

Work supported by
the U.S. Department of Energy
under DE-AC03-99ER54463

GENERAL ATOMICS PROJECT 30033
JULY 2003

Validation of the Physics Model for ECCD in the DIII-D Tokamak and its Application to ITER

R. Prater, C.C. Petty, R.W. Harvey[#], J.M. Lohr, T.C. Luce, M. Choi

General Atomics, San Diego, California
[#]CompX, Del Mar, California

1. Introduction

Accurate projection of the magnitude and profile of electron cyclotron current drive (ECCD) in ITER requires the experimental validation of a predictive physics model. Experiments [1-3] have been undertaken in the DIII-D tokamak to validate the first-principles physics models encoded in the TORAY-GA [4,5]/CQL3D [6] suite of codes. This comparison shows that the computational model provides excellent predictive capability for the parameter range available in the experiments.

In this paper, we present the comparisons of the codes with the experimental measurements. Based on the agreement, we apply with confidence the TORAY-GA code to the ITER equilibrium. The code addresses the competition between the two components of the ECCD, namely the Fisch-Boozer (FBCD) [7] and Ohkawa (OKCD) [8] components. Applying the code to the case of midplane launch in order to emphasize the Ohkawa current as suggested by Decker [9], we find that under the reference conditions the FBCD always dominates due to the large optical depth in the ITER plasma. Applying the code instead to the reference launcher location near the top of ITER, the optimum conditions for current drive near the q=3/2 and q=2 rational surfaces can be determined.

2. Validation of the Computational Model for ECCD

The TORAY-GA ray tracing code [4,5] calculates the trajectories of a bundle of rays which simulate the propagation of a Gaussian beam far from the beam waist. For the DIII-D study, we use 30 rays with a characteristic divergence of 1.7 deg at half power. The code calculates the wave absorption and the current drive using the Cohen model [5]. For more accurate modeling, the ray trajectories and the wave polarizations from TORAY-GA are used as input to the CQL3D bounce-averaged Fokker-Planck code [6] in order to include quasilinear effects of the wave and the effects of the parallel electric field $E_{||}$ (which drives the Ohmic current) on the distribution function. The calculated ECCD can be compared with the current measured in experiments on the DIII-D tokamak.

The DIII-D experiments use measurements from the motional Stark effect (MSE) diagnostic [10] to measure the pitch angle of the magnetic field with radial resolution around 5 cm over much of the minor radius. An extensive set of experiments has been carried out in which the minor radius, the parallel index of refraction, and the poloidal location of the interaction are varied in an orthogonal manner, as well as the plasma parameters like electron temperature and density [1]. In order to accurately model the physics, the effects of the radial profile of the self-consistent toroidal electric field must be included, where the electric field is obtained from the evolution of the magnetic flux in a series of equilibrium reconstructions constrained by the MSE data [11].

The magnitude of the measured ECCD plotted against the ECCD calculated by the CQL3D code for the complete experimental database shows excellent agreement, as shown in Fig. 1(a) [2]. Measurements of the profile peak and width are also in excellent agreement between experiment and theory. Even in high performance discharges with edge localized modes

(ELMs), sawteeth, and tearing modes present, the width of the profile of driven current does not seem to be measureably wider than that calculated with no MHD activity assumed [3]. The principal limitations on the data set shown in the figure are that the maximum normalized minor radius is 0.4, while applications in DIII-D and ITER will require ECCD at radii of 0.5 to 0.8 where trapping of electrons is stronger, and the electron temperature is less than 5 keV in this dataset.

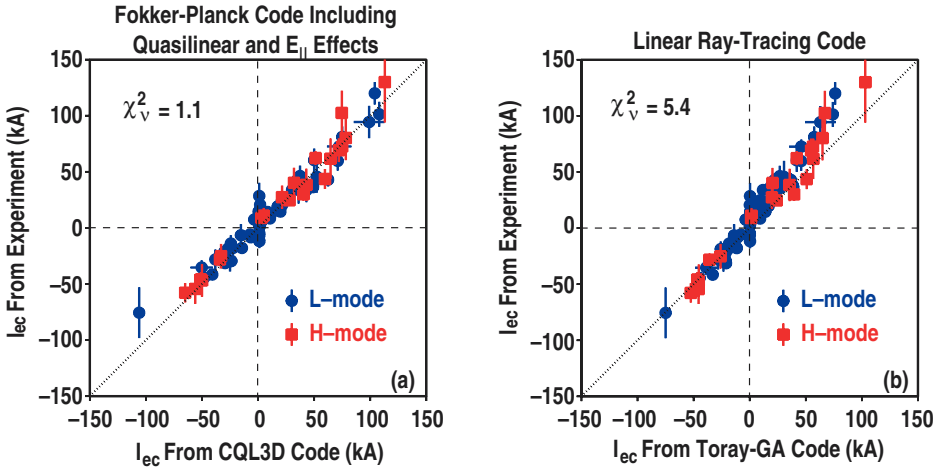

Fig. 1. The measured ECCD current for the entire database of ECH discharges in DIII-D versus the current calculated by (a) the CQL3D Fokker-Planck code including the effect of the parallel electric field and (b) the TORAY-GA code. The blue circular data points are for L-mode and the red squares are for H-mode discharges with higher temperature and density.

The ECCD calculated by TORAY-GA is also an acceptably good fit to the measurements, as shown in Fig. 1(b). The deviations are largest at the largest driven current, but it seems that this is not a result of quasilinear effects. Harvey [12] derived the criterion that for $Q_e(MW/m^3)/n_e^{\zeta}(10^{19}\ m^{-3}) < 0.5$ significant quasilinear deviations from should not be expected, where Q_e is the EC power density and n_e is the particle density. The ratio of the measured ECCD to the ECCD calculated by CQL3D and TORAY-GA for the database from Fig. 1 is plotted in Fig. 2 as a function of this criterion. No clear deviation in the current ratio can be correlated with the quasilinear criterion over the range available. We conclude from this that the deviation of the experiment from the TORAY-GA calculation must be due primarily to the effects of $E_{||}$, which is not included in the calculations with TORAY-GA. For ITER the $E_{||}$ will be very small. Additionally, the Q_e/n_e^{ζ} for ITER is an order of magnitude smaller than the criterion [3], so quasilinear effects should be fully negligible. We conclude that TORAY-GA calculations should be valid for the plasmas in ITER.

3. OKCD in ITER

Decker, Peysson, Bers, and Ram [9] have suggested that high current density far off-axis can be supplied by ECCD by launching in a way which optimizes the Ohkawa current rather than the Fisch-Boozer current. Since in the OKCD technique the power would be applied ideally at the bottom of the magnetic well near the outboard midplane, this could be an ideal launching condition with the additional benefit of reduced requirements on the frequency of the ECH source. The physics feasibility of this technically attractive option was tested for ECCD near the q = 2 surface for an equilibrium similar to the ITER Scenario 2 equilibrium.

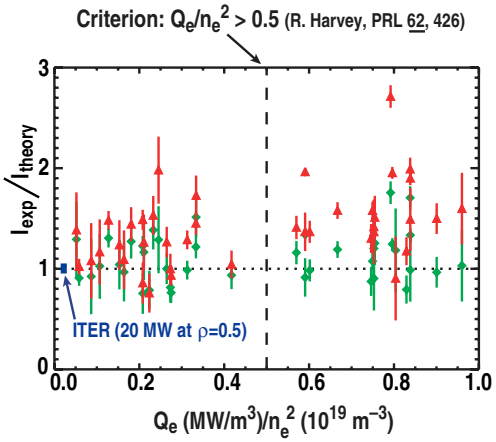

Fig. 2. The ratio of measured ECCD to that calculated by CQL3D (green diamonds) and by TORAY-GA (red triangles) for the data from Fig. 1 plotted against the quasilinear reference quantity $Q_e(MW/m^3)/n_e(10^{19}\ m^{-3})$. The Harvey criterion is the dashed vertical line. The Q_e/n_e^2 projected conservatively for ITER is also shown.

To test the idea of emphasizing OKCD the TORAY-GA code was used to evaluate the current drive using a midplane launch, the optimum location for the OKCD. The first calculations were done for DIII–D geometry and parameters, except that the launcher was moved (computationally) to the outboard midplane to maximize the OKCD, using the second harmonic X-mode for which the frequency is considered a free parameter. The key parameters which affect the current drive are the local values of $n_{||}$, θ_{pol}, and ε. Here, $n_{||}$ is the parallel index of refraction, θ_{pol} is the poloidal angle which runs from zero at the outboard midplane to 180 degrees at the inboard midplane, and ε is the inverse aspect ratio. The parameters θ_{pol} and ε uniquely define the location of the absorption in the (R, Z) plane. Typical L-mode kinetic profiles were used for density and temperature. The $\rho = 0.76$ case ($q = 2$) corresponds to $\varepsilon = 0.293$ for the equilibrium used (#103969.01600), and the kinetic profiles were multiplied by a constant such that at the $q = 2$ surface the electron temperature $T_e = 2$ keV and the electron density $n_e = 2.0\text{x}10^{19}\text{m}^{-3}$. Z_{eff} was constant at 2.0. An appropriate range of $n_{||}$ from –0.6 to 0.6 was used. For each $n_{||}$ the rf frequency was adjusted until the absorption was peaked at the desired location in physical space.

The first case treated was for interaction at θ_{pol} near 180° (inboard midplane), which corresponds to the optimum location on the flux surface for FBCD and which minimizes the OKCD since the trapping region in velocity space is minimized. This case is not physically realizable for DIII–D or any other moderately low aspect ratio tokamak because significant absorption will take place at higher harmonics lying within the plasma. Nevertheless, currentdrive at this location serves as a useful fiducial for other physically realizable cases. So in this study absorption was calculated only for the second harmonic. The results of a scan of $n_{||}$ are shown in Fig. 3. About 23 kA/MW are obtained at the maximum $n_{||}$ tested of 0.6, as shown in Fig. 3(a). For the DIII-D geometry and sign of B_t (negative), this corresponds to FBCD. However, as $n_{||}$ increases the radial thickness of the absorption also increases due to increased Doppler broadening by more than the current increases, so the driven current density peaks at an intermediate value of $n_{||}$ of 0.28. Figure 3(b) shows this effect, with the maximum current. density of11.3 A/cm^2/MW. The source frequency which provides the optimum current density is 162.2 GHz at $n_{||}$=0.28.

On the other hand, applying the ECCD at θ_{pol} near 0 degrees (outboard midplane) does in fact show a predominance of the OKCD, as shown in Fig. 4. The sign of the driven current in

Fig. 4(a) is inverted from that of Fig. 3(a), with the maximum driven co-current at $n_{||}$ = -0.24. The maximum current density, Fig. 4(b), has a sharp peak with 7.8 A/cm^2/MW at the same $n_{||}$. This current density is ≈70% that of Fig. 3, the ideal but physically unrealizable FBCD case. The source frequency required for this case is 87.3 GHz. This may make an attractive way of driving ECCD far off-axis in a device like DIII-D, with reduced frequency and with convenient midplane launch, as pointed out by Decker.

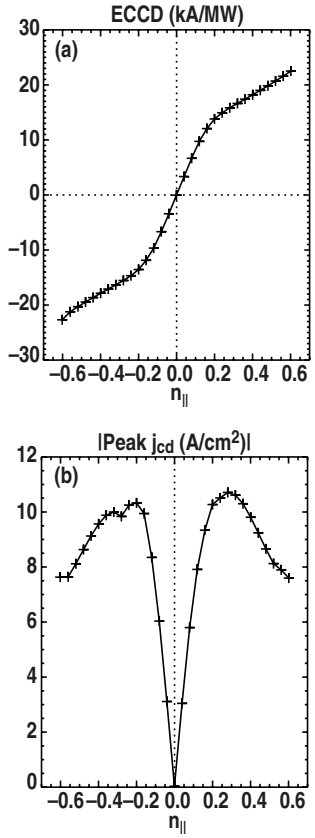

Fig. 3. (a) Driven current and (b) absolute value of peak current density as a function of the local n_l determined at the location of the peak rate of absorption of the central ray. The equilibrium is DIII-D, with peak driven current at ρ=0.76, and the interaction is placed at the inboard midplane. The local T_e=2 keV, n_e=2x10^{19} m^{-3}, and Z_{eff}=2. The applied frequency is 162.2 for the n_l=0.28 case. In this condition FBCD dominates.

EECD for ITER was evaluated on a Scenario 2-like equilibrium with plasma current of 15 MA and toroidal field of magnitude 5.3 T at a nominal major radius of 6.2 m. The local electron temperature at ρ = 0.75 where the current drive takes place is 7.1 keV and the density is 1.04 x 10^{20} m^{-3}. For the tests of FBCD vs OKCD the ECH launcher was placed at the outboard side of the plasma at the approximate elevation of the magnetic axis. The O-mode fundamental was used. An array of 30 rays simulates a Gaussian beam with divergence of 1.17 deg HWHM, corresponding to the design of the ECH launcher for ITER.

For a comparison point, the first computations were again done for ECH deposition at the inboard midplane where trapping should be minimum. Again, this situation is not accessible experimentally in ITER because the absorption at the second harmonic near the center of the plasma would be overwhelming. In this study the second harmonic absorption was suppressed in the computation.

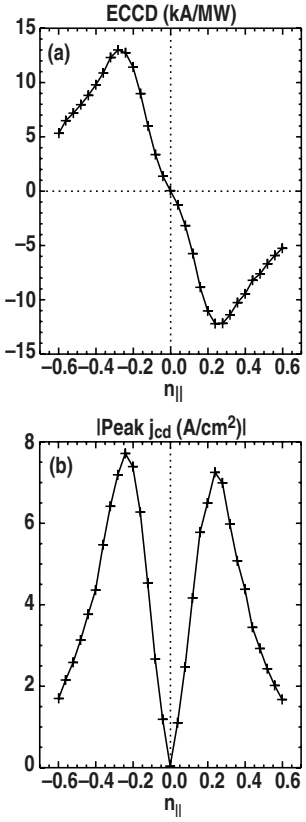

Fig. 4. Same as Fig. 3, but the interaction is placed at the outboard midplane and the applied frequency for the $n_{\|}$=-0.24 case is 87.3 GHz. OKCD dominates for this situation.

Figure 5(a) shows that FBCD predominates, as expected. (Recall that the sign of B_t is opposite that of DIII–D, so the sign of $n_{\|}$ must be inverted for comparison with DIII–D modeling.) The peak driven current is 13 kA/MW at $n_{\|}$ = -0.6. The peak current density is 0.38 A/cm^2/MW, which occurs at $n_{\|}$ = -0.44, shown in Fig. 5(b). In this case the required source frequency is 221.3 GHz.

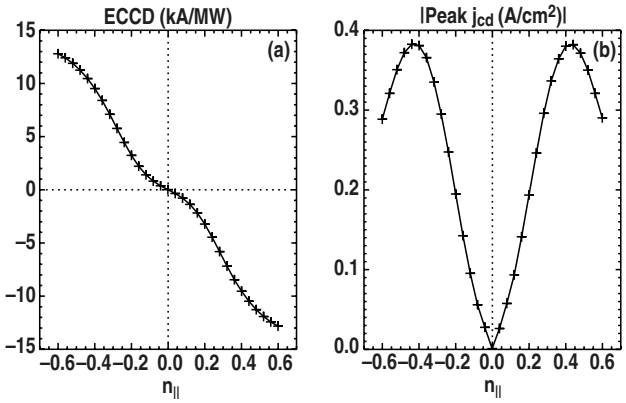

Fig. 5. (a) Driven current and (b) absolute value of peak current density as a function of the local $n_{\|}$ determined at the location of the peak rate of absorption of the central ray. The equilibrium is ITER Scenario 2 with peak driven current at ρ=0.76, and the interaction is placed at the inboard midplane. The local T_e=7.1 keV, n_e=1.02x10^{20} m^{-3}, and Z_{eff}=1.5. The applied frequency is 221.3 for the $n_{\|}$=-0.44 case.

The comparison ITER case with absorption at the outboard midplane also shows dominantly FBCD for all $n_{||}$. This is shown in Fig. 6. The peak driven current is 5.63 kA/MW, about half of the current driven at the inboard side, at $n_{||}$ = -0.48. The peak driven current density is 0.193 A/cm^2/MW, which takes place at nearly the same $n_{||}$ = –0.44. The frequency is relaxed, however, to 140 GHz.

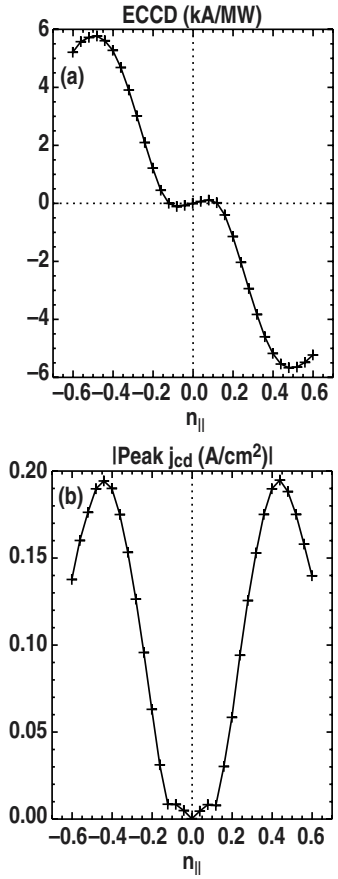

Fig. 6. Same as Fig. 5, but the interaction is placed at the outboard midplane and the applied frequency for then$_{||}$=-0.44 case is 140.6 GHz.

The root of the difference between the dominance of the OKCD in outboard ECCD on DIII–D and the dominance of the FBCD in outboard ECCD on ITER can be seen in the expression for the optical depth. As the optical depth increases the wave absorption takes place further from the cold resonance. The optical depth [13] is proportional to the product $(n_e/n_c)(T_{keV}/511)(L_B/\lambda)$, where n_c is the density given by $\omega_p^2 = \omega_c^2$ or $n_c\,(m^{-3}) = 1.2\text{x}10^{16}\,f^2\,(GHz) = 0.974\text{x}\,10^{19}\,B^2(T)$, $L_B = B/(dB/ds)$ is the scale length over which the magnetic field changes along the ray trajectory, and $\lambda = 2\pi c/\omega$ is the free-space wavelength. In this study, the value of (n_e/n_c) for DIII–D was similar, but the ratio of T_e for ITER to that of DIII–D was a factor 3.5. However, most important is the factor L_B/λ, which is 5.5 times larger for ITER than for DIII–D. So for ITER the optical depth is over 100 while for DIII–D it is around 10. This large difference, which is attributable mainly to the size of ITER relative to the wavelength, causes the power to be absorbed far from the resonance in ITER, so that trapping will be minimized. The implication of this is that the case of dominant OKCD is not accessible for ITER except possibly very near the edge, but also that the effect of trapping is a modest factor of 2.

4. Benchmarking for ITER

An ECH launcher in the upper part of the ITER vacuum vessel has been designed for the purpose of stabilization of neoclassical tearing modes. The experimentally validated physics model for ECCD can be applied to this case to determine the effectiveness of the reference launcher location for driving current near the rational q surfaces. The physical location of the launcher at R=6.485 m and Z=4.110 m is shown on the cross-section of the Scenario 2 equilibrium in Fig. 7 (eqdsk file g2_129x129.dat). The fundamental resonance for 170 GHz, the nominal frequency choice for ITER, is also shown, as well as some low-order rational q surfaces.

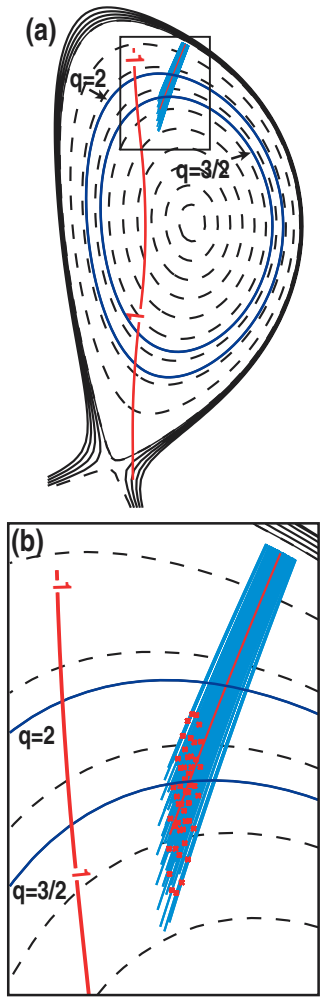

Fig. 7. (a) ITER Scenario 2 equilibrium g2_129x129.dat, with the 170 GHz fundamental electron cyclotron resonance shown. Also shown are the ECH launcher location and an array of rays. (b) Expansion of the area in the box in (a). The red dots signify the peak in dP/ds for each ray.

The TORAY-GA code has been used to model current drive for this equilibrium, using the kinetic profiles from the Scen2.xls file on the ITER website. The EC beam is modeled as an array of 48 rays emitted from a point source with Gaussian divergence angle 1.177 deg for half angle at half power. The effective launch location is moved away from the plasma by 2.03 m along the ray direction to simulate a beam radius of 7.1 cm at the actual launch location. The angles of the ray bundle launched from this antenna are characterized by the angles α and β,

where α is the angle between the horizontal plane and the poloidal component of the nominal beam centerline and β is the angle between the nominal beam centerline and its poloidal component. Then α and β are related to the polar angle θ and the azimuthal angle ϕ (the conventional Euler angles) used by TORAY-GA through the relationships $\theta = \mathrm{acos}(\cos(\beta)\sin(\alpha))$ and $\phi = \pi + \mathrm{asin}(\sin(\beta)/\sin(\theta))$.

In order to systematically study the effectiveness of ECCD using this launcher the control angles α and β were scanned through a matrix of values corresponding to a reasonable range, given this geometry. The applied frequency was held fixed at 170 GHz. In Fig. 8 the contours of ρ, the normalized minor radius of the peak rate of current deposition along a ray, are plotted as the blue contours, along with the minor radii corresponding to q=3/2 and q=2 (green contours). Also shown in this plot are the contours of the magnitude of the driven current, in kA/MW (red contours). For the q=3/2 surface the peak driven current is about 12 kA/MW obtained for β=-27 deg, while for the q=2 surface the maximum driven current is about 9 kA/MW for β=-28 deg.

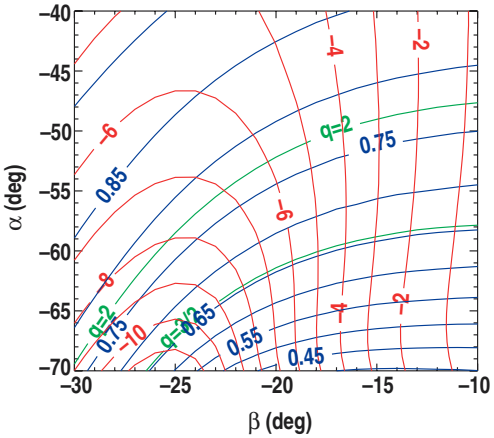

Fig. 8. Contours of I_{ECCD}/P (kA/MW) (red curves), normalized minor radius of peak current drive (blue), and rational q surfaces (green), as functions of launch angles alpha and beta.

The contours of current density are shown in Fig. 9. These values are obtained by fitting the radial profile of driven current to a Gaussian and using the peak of the fitted distribution. This process is needed because the radial grid size used for ρ in the transport code has 51 points. The width of the ECCD is in some cases only 3 or 4 radial grid points wide. This necessitates a fitting procedure to avoid the random noise which would be found with a procedure just using the largest value at some grid point. In practice the Gaussian fit is rather accurate. There is a distinct maximum in j_{ECCD} at the q=3/2 surface of ≈0.26 A/cm^2/MW at α=-66 deg and β=-24 deg, while j_{ECCD} at the q=2 surface has a maximum of 0.28 A/cm^2/MW at α=-55 deg and β=-22.6 deg. The ray trajectories for the case of optimum current density at the q=3/2 surface are shown in Fig. 7. Because the rays approach the resonance obliquely the absorption takes place over an arc length of >30 cm, and this width is mostly responsible for the broadening of the current drive profile. It is notable that for this geometry the maximum current density at the q=2 surface is larger than that at the q=3/2 surface. Even though the total current is smaller at the q=2 surface, the width of the profile of driven current is smaller due to the geometry. This is seen in Fig. 10, which shows the profile width as a function of launch angles. The minimum Δρ is ≈0.1, which is rather large, and at the maximum of j_{ECCD} is 0.14.

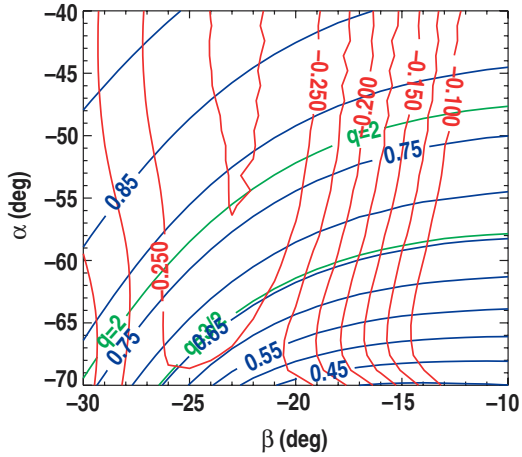

Fig. 9. Contours of j_{ECCD}/P (A/cm^2/MW) (red curves), normalized minor radius of peak current drive (blue), and rational q surfaces (green), as functions of launch angles alpha and beta.

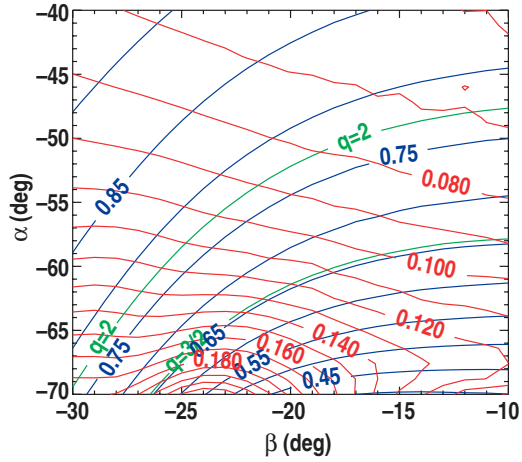

Fig. 10. Contours of the width of the current drive Δρ (red curves), normalized minor radius of peak current drive (blue), and rational q surfaces (green), as functions of launch angles alpha and beta. Δρ is full width at 1/e power.

Any launcher for the purpose of driving current near the outer parts of the plasma should satisfy the requirements: 1) the location of the driven current over a range of rho centered about the targeted flux surface should be determined by the launch angles of the ECH beam without extreme sensitivity or insensitivity to the launch angles; 2) the total driven current should be near the maximum possible for that flux surface (this means fairly near the high field side of the flux surface); 3) the width of the current deposition layer should be minimum and comparable to or less than the island width, and it appears that this means that the beam width rather than the absorption length should determine the deposition width; and 4) absorption at unwanted harmonics should be minimum.

The proposed location of the launcher near the top of the discharge meets these criteria only moderately well. Figure 9 shows that the ρ of the peak of the driven current can be changed by changing primarily the angle α without strongly changing the driven current or the

width of the driven current profile. However, the peak in j_{ECCD} takes place at angles for which the $\Delta\rho$ is unacceptably large.

There are several approaches to improving the launcher effectiveness. First, improved optics (i.e.,narrower beam) can help narrow the profile of driven current. A study similar to that of Figs. 8 through 10 but using a point source launch at the actual launch location instead of 2.1 m away from the plasma suggests that above 0.4 A/cm^2/MW can be obtained at the q=2 surface, a 50% increase. Narrowing the beam divergence would also help and would seem to be possible. Raising the source frequency to 180 to 192 GHz also sustantially improves the peak j_{ECCD} and more importantly decreases $\Delta\rho$ to something close to the actual beam width. Alternatively, lowering the launcher location would help.

Acknowlegement

This is a report of work supported by the U.S. Department of Energy under Contract No. DE-AC03-99ER54463 and in part by General Atomics IR&D funding.

References

[1] C.C. Petty, R. Prater, J. Lohr, et al., Nucl. Fusion **42**, 1366 (2002).
[2] C.C. Petty, R. Prater, T.C. Luce, et al., "Physics of Electron Cyclotron Current Drive on DIII-D," in Proc. of the 19th IAEA Fusion Energy Conference, Lyon, France, 2002 (International Atomic Energy Agency, Vienna).
[3] R. Prater, C.C. Petty, T.C. Luce, R.W. Harvey, et al., "Electron Cyclotron Curent Drive in DIII-D: Experiment and Theory," General Atomics Report GA-A24340 (2003), to be published in Radio Frequency Power in Plasmas, 15th Topical Conference, Moran, Wyoming.
[4] K. Matsuda, IEEE Trans. Plasma Sci. **17**, 6 (1989).
[5] R. Cohen, Phys. Fluids **30**, 2442 (1987).
[6] R.W. Harvey and M.G. McCoy, in Proc. of the IAEA Technical Committee Meeting, Montreal, 1992 (IAEA, Vienna, 1993) 498.
[7] N.J. Fisch and A.H. Boozer, Phys. Rev. Letters **45**, 720 (1980).
[8] T. Ohkawa, "Steady-State Operation of Tokamaks by R-F Heating," General Atomics Report GA-A13847 (1976).
[9] J. Decker, Y. Peysson, A. Bers, A.K. Ram, Proc. 12th Joint Workshop on Electron Cyclotron Emission and Electron Cyclotron Heating, Aix-en-Provence, 13-16 May 2002 ed. G. Giruzzi (World Scientific, New Jersey, 2002), p. 113.
[10] B.W. Rice, K.H. Burrell, L.L. Lao, Y.-R. Lin-Liu, Phys. Rev. Letters **79**, 2694 (1997).
[11] C.B. Forest, K. Kupfer, T.C. Luce, et al., Phys. Rev. Lett. **73**, 2444 (1994).
[12] R.W. Harvey, M.G. McCoy, G.D. Kerbel, Phys. Rev. Letters **62**, 426 (1989).
[13] M. Bornatici, R. Cano, O. De Barbieri, F. Engelmann, Nucl. Fusion 9, 1153 (1983).